AGU PUBLICATIONS

Geophysical Research Letters

RESEARCH LETTER

10.1002/2017GL073499

Key Points:
- Taylor's hypothesis does not apply in the atmospheric surface layer
- Instead of being constant, the convective velocity exhibits a $k^{-1/3}$ dependence at high wave numbers in the inertial subrange
- A correction is proposed for eddy-covariance measurements

Supporting Information:
- Supporting Information S1

Correspondence to:
Y. Cheng,
yc2965@columbia.edu

Citation:
Cheng, Y., C. Sayde, Q. Li, J. Basara, J. Selker, E. Tanner, and P. Gentine (2017), Failure of Taylor's hypothesis in the atmospheric surface layer and its correction for eddy-covariance measurements, *Geophys. Res. Lett.*, *44*, 4287–4295, doi:10.1002/2017GL073499.

Received 17 MAR 2017
Accepted 12 APR 2017
Accepted article online 18 APR 2017
Published online 4 MAY 2017

Failure of Taylor's hypothesis in the atmospheric surface layer and its correction for eddy-covariance measurements

Yu Cheng[1], Chadi Sayde[2,3], Qi Li[1], Jeffrey Basara[4], John Selker[2], Evan Tanner[5], and Pierre Gentine[1]

[1]Department of Earth and Environmental Engineering, Columbia University, New York, New York, USA, [2]Department of Biological and Ecological Engineering, Oregon State University, Corvallis, Oregon, USA, [3]Now at the Department of Biological and Agricultural Engineering, North Carolina State University, Raleigh, North Carolina, USA, [4]School of Meteorology, University of Oklahoma, Norman, Oklahoma, USA, [5]Department of Natural Resource Ecology and Management, Oklahoma State University, Stillwater, Oklahoma, USA

Abstract Taylors' frozen turbulence hypothesis suggests that all turbulent eddies are advected by the mean streamwise velocity, without changes in their properties. This hypothesis has been widely invoked to compute Reynolds averaging using temporal turbulence data measured at a single point in space. However, in the atmospheric surface layer, the exact relationship between convection velocity and wave number k has not been fully revealed since previous observations were limited by either their spatial resolution or by the sampling length. Using Distributed Temperature Sensing (DTS), acquiring turbulent temperature fluctuations at high temporal and spatial frequencies, we computed convection velocities across wave numbers using a phase spectrum method. We found that convection velocity decreases as $k^{-1/3}$ at the higher wave numbers of the inertial subrange instead of being independent of wave number as suggested by Taylor's hypothesis. We further corroborated this result using large eddy simulations. Applying Taylor's hypothesis thus systematically underestimates turbulent spectrum in the inertial subrange. A correction is proposed for point-based eddy-covariance measurements, which can improve surface energy budget closure and estimates of CO_2 fluxes.

1. Introduction

Application of Taylor's frozen turbulence hypothesis of the exchangeability of time and space in characterizing turbulence [*Taylor*, 1938] has been an essential step in calculating Reynolds averaging from point temporal data to retrieve atmospheric surface turbulent fluxes (momentum, heat, water vapor, and CO_2) [*Kaimal et al.*, 1972]. These computed fluxes in turn have been used to constrain land surface, weather forecast, and climate models and are thus key for improved hydrological, weather, climate, and carbon cycle prediction [*Mueller et al.*, 2013; *Mueller et al.*, 2011]. The common interpretation of Taylor's hypothesis is that it assumes that turbulence is "frozen"; i.e., the eddy property is not changing during advection, and that all eddies are advected at the mean flow velocity. As a result, it is taken to be justified to employ point measurement of temporal fluctuations in lieu of spatial fluctuations and Reynolds averaging.

Because of the fundamental role of Taylor's hypothesis in transforming commonly available temporal data into typically inaccessible spatial turbulent data, many studies have been conducted questioning its validity and its limitations using theory [*Lin*, 1953; *Lumley*, 1965; *Wyngaard and Clifford*, 1977], field measurements [*Higgins et al.*, 2012; *Mizuno and Panofsky*, 1975; *Tong*, 1996], or laboratory studies [*Burghelea et al.*, 2005; *Buxton et al.*, 2013; *Dennis and Nickels*, 2008; *Fisher and Davies*, 1964].

Taylor's hypothesis, when considered in spectral space and in one dimension along the streamwise velocity, means that the spatial wave number spectrum can be computed using the single-point time frequency spectrum [*Wyngaard and Clifford*, 1977]:

$$F_{11}(k_1) = \bar{U}\, W_{11}\left(k_1 \bar{U}\right), \tag{1}$$

where k_1 the is streamwise wave number in one dimension, $F_{11}(k_1)$ is the one-dimensional wave number spectrum, $\bar{U}$ is the mean streamwise wind velocity in the streamwise (x_1) direction, W_{11} is the frequency spectrum and the subscript 1 denotes the spatial direction (See details of derivation in the supporting information).

In other words, Taylor's hypothesis assumes that there is a single frequency corresponding to one particular wave number (i.e., there is a one-to-one correspondence between wave number and frequency spectrum) and that the frequency is proportional to the wave number and related to the mean streamwise velocity by $\omega = k_1 \bar{U}$ (We note that ω and $k_1 U$ have the same units). Experiments [*Fisher and Davies*, 1964; *Tong*, 1996] have shown that Taylor's hypothesis fails if eddies of different sizes travel at different velocities, in which case turbulent wave number spectrum cannot be simply interpreted as the frequency spectrum.

The convection velocities of different wave numbers can be calculated from wave number frequency spectrum [*Wills*, 1964], local derivative of spectrum [*Del Álamo and Jiménez*, 2009], and phase spectrum [*Buxton et al.*, 2013; *Powell and Elderkin*, 1974]. Some results relating convection velocity and wave number have been obtained [*Atkinson et al.*, 2015; *Buxton et al.*, 2013; *de Kat et al.*, 2013; *Del Álamo and Jiménez*, 2009; *Fisher and Davies*, 1964; *Goldschmidt et al.*, 1981; *Higgins et al.*, 2012; *Kim and Hussain*, 1993], but no quantitative relation between convection velocity and wave number has been reported since most data have been limited by either spatial resolution (hence, separation with Kolmogorov microscale) or sample length (hence, Reynolds number). Yet overall, the main conclusion seems to be that larger eddies are reported to convect at larger velocity than smaller eddies, at least near the wall [*Atkinson et al.*, 2015; *Chung and McKeon*, 2010; *Del Álamo and Jiménez*, 2009; *Krogstad et al.*, 1998].

At flux tower sites, the surface energy budget has typically not been able to close due to an apparent underestimation of turbulent heat fluxes [*Foken*, 2008; *Foken et al.*, 2010]. Further, it was recently pointed out that the cospectra corrections may cause significant changes in CO_2 fluxes [*Mamadou et al.*, 2016] due to the impact of small eddy size (high wave number) cospectrum on the overall long-term CO_2 fluxes.

We here reinvestigate Taylor's hypothesis using temperature data obtained from Distributed Temperature Sensing (DTS) at high temporal and spatial frequency in the atmospheric surface layer. These data are complemented by results from large eddy simulations (LES) of an unstable atmospheric boundary layer over smooth and rough surfaces. The present manuscript reveals a $k^{-1/3}$ dependence of convective velocity at high wave numbers in the inertial subrange. The application of Taylor's hypothesis is then shown to systematically underestimate the wave number spectrum in the inertial subrange, which may be among the causes of underestimation of surface energy turbulent fluxes. A correction for time-domain turbulent measurements is then proposed.

2. Materials and Method

2.1. Experiment Setup

DTS utilizes the ratio of Stokes and anti-Stokes of Raman scattering in an optic fiber. Commercial instruments can obtain temperature continuously at resolution of 0.01°C, every meter, over distances of up to 10,000 m [*Selker et al.*, 2006a]. DTS has been extensively applied in environmental monitoring [*Becker et al.*, 2013; *Briggs et al.*, 2012; *Selker et al.*, 2006a, 2006b; *Tyler et al.*, 2009]. It has also been useful in the atmospheric boundary to investigate turbulent structures [*Sayde et al.*, 2015; *Thomas et al.*, 2011; *Zeeman et al.*, 2015]. For this study a DTS system (Ultima S, Silixa Ltd, Hertfordshire, UK) was installed at the Oklahoma State University Range Research Station, Stillwater, OK, from 20 May to 15 July 2016. The land surface was mostly flat with some microtopography and was covered with growing grass typically shorter than 30 cm. Fiber optics (FO) were set up at four heights (1.00 m, 1.25 m, 1.50 m, and 1.75 m above ground) parallel to the ground to build a 233 m long transect in the direction of 50° north of east (Figure 1). The FO cables (AFL Telecomm NSX001509U601-BIF, Graybar, NY, USA) were white in color with an OD of 0.0009 m. The 18 tripods separated by 13.7 m supported the FO cables. The tensioning systems, consisting of suspended adjustable weights, were attached to the cables at the end of the transect to maintain constant tension on the cables so that the cables remain stretched and parallel to each other while avoiding excessive tension (approximately 15 N). At each end of the FO cable two calibration baths (one cold and one warm) were established to calibrate the DTS readings (Figure 1). About 20 m of FO, cable were held in each calibration bath. Ice was added periodically to the cold bath, in order to maintain a constant temperature close to 0°C. The warm bath was left at ambient temperature. An air bubbler was installed at each calibration bath to circulate water and avoid thermal stratification. RBRsolo temperature sensors (NIST certified to 0.002°C accuracy, RBR Ltd Ottawa, Canada) were used to precisely monitor the bath temperatures. The temperatures collected by the DTS were sampled every 0.127 m in space and every 1.5 s time, though the fundamental resolution of the

10.1002/2017GL073499

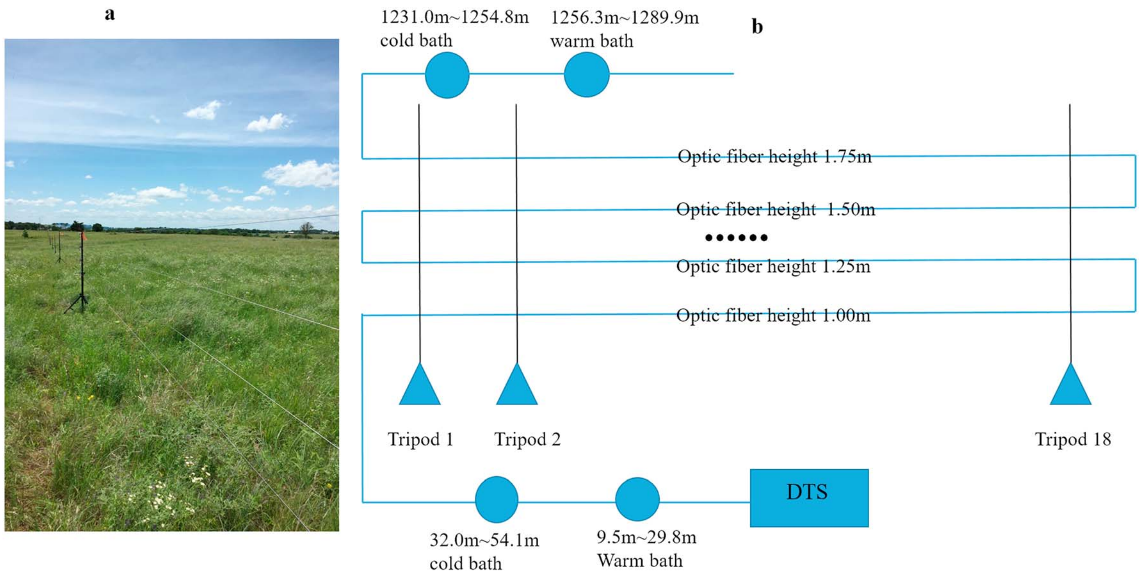

Figure 1. (a) Picture of the installation at the Oklahoma State University Range Research Station site. Four parallel 233 m long fiber optics were maintained by tripods to measure air temperature. (b) Schematic of the DTS transect and of the fiber optics setup. The four water baths were used to calibrate the fiber temperature.

DTS is rated as 0.29 m. The Obukhov length was derived from the eddy covariance tower, owned by University of Oklahoma, located within 5 m of the end of the fiber transect. An Oklahoma Mesonet weather station located approximately 150 m east of the transect was used to provide meteorological conditions.

In addition to the DTS data, we used high-resolution large eddy simulation (LES) to further confirm our theoretical results and investigate the impact of the surface roughness. High-resolution LES can correctly capture the inertial subrange [*Sullivan and Patton*, 2011]. The LES data were used to test the validity of our findings for momentum in addition to temperature. The LES simulations are also used to further validate the observation results, which are prone to measurement errors.

The setup of the LES is only briefly described here, as further computational details and the subgrid-scale (SGS) model were presented in previous studies [*Albertson*, 1996; *Bou-Zeid et al.*, 2005; *Kumar et al.*, 2006; *Porté-Agel et al.*, 2000]. In the LES, the filtered mass conservation equation, Navier-Stokes equations with Boussinesq approximation and the temperature (as a conserved scalar) advection-diffusion equation was solved using a pseudospectral method in horizontal directions and a second-order centered finite difference in vertical direction. The dynamic Lagrangian scale-dependent SGS model [*Bou-Zeid et al.*, 2005] was used, and a constant SGS Prandtl number of 0.4 was applied. The physical dimensions of the domain is $L_x \times L_y \times L_z = 6.28 \times 6.28 \times 1.5$ (km^3) with the number of grid points being 256 in each direction. A constant and spatially uniform surface heat flux of 0.05 K m s^{-1} was imposed. A geostrophic forcing of $(u_g, v_g) = (8, 0)$ ms^{-1} drove the velocity field with the Coriolis parameter being 1.394×10^{-4} s^{-1}. We used the Monin-Obukhov similarity theory [*Monin and Obukhov*, 1954] in the first grid level to compute the surface stress. This is a common approach used in high Reynolds number boundary layer flows, where the viscous sublayer is not resolved [*Moeng*, 1984; *Sullivan and Patton*, 2011]. Furthermore, we adopted the same method in *Bou-Zeid et al.* [2005] and *Kumar et al.* [2006] in which the velocity filtered at twice the filter size was used here. Two cases with different roughness length z_{0m} were simulated. One case had a constant $z_0 = 0.01$ m, which was referred to as the "rough" case. The z_0 of the second case, referred as the smooth case, was dynamically calculated using $\nu/9u^*$ assuming the surface was aerodynamically smooth [*Li et al.*, 2016].

The LES data were recorded in an array of "virtual sensors" [*Cancelli et al.*, 2014] akin to the DTS in the field measurements. The "virtual sensors" with $n_x \times n_y \times n_z = 256 \times 1 \times 5$, where n_x, n_y, and n_z are the number of points in each direction, respectively, were positioned along x (downwind direction) at one crosswind location of $y = 0.5L_y$ at five different vertical levels that spanned 10% of z_i, which corresponded approximately to the surface layer height. To be comparable to the DTS measurement, the recorded data had a frequency of

1 Hz (the output was at every twentieth time step since the time step in LES was 0.05 s). In total, 2000 s of data were used for the analysis. Temporal fluctuations were compared to spatial variations along the streamwise directions, at the first model level where the subgrid-scale contribution to the fluxes was smaller than 3% of the total resolved fluxes, to avoid any subgrid-scale influence on the results.

2.2. Calculation of Convection Velocity

For each one-dimensional wave number k_1, the convection velocity was computed using the phase spectrum method as

$$U(k_1) = \frac{\Delta\varphi}{k_1 \times \Delta t}, \tag{2}$$

where $U(k_1)$ is the wave number-dependent convection velocity, $\Delta\varphi$ is the phase difference of Fourier transform of velocity between time t and $t + \Delta t$. The phase spectrum method was used to calculate wave number-dependent convection velocity (see *Buxton and Ganapathisubramani* [2011] and *Buxton et al.* [2013] for details), because large eddies may influence the estimate of smaller eddies in space-time correlation and amplitude estimates [*Zhao and He*, 2009]. Here the phase difference of the Fourier transform of the space-time temperature data was used to represent the convective velocity, as Taylor's hypothesis can be applied to any scalar.

3. Data

Nine representative 30 min periods (28 May 05:15–05:45 A.M. CST, 28 May 02:05–2:35 A.M. CST, 5 June 5:15–5:45 P.M. CST, 2 June 9:15–9:45 A.M. CST, 29 May 11:50 A.M. −12:20 P.M. CST, 2 June 9:55–10:25 A.M. CST, 29 May 9:00–9:30 A.M. CST, 28 May 09:45–10:15 A.M. CST, and 28 May 1:15–1:45 P.M. CST) were selected when wind direction was along (parallel to) the optic cable (eight periods were within 10° of the cable and one was within 13°). First, a smoothing filter was applied to remove the white noise generated by DTS at high frequencies. The smoothing filter calculated the moving average of two nearby temperatures in both time and space. Therefore, the effective DTS spatial resolution was 0.56 m. The effective temporal resolution was 3 s. A "spatial average" filter was then applied to calculate the mean temperature of every six spatial points. The temperature resolution was 0.16°C and 0.22°C before and after transect, respectively, which was calculated from the calibration baths using the standard deviation of bath temperature. The data that were treated only with "spatial average" filter are called "averaged data", while the data that were treated with both smoothing and "spatial average" filters are called "smoothed and averaged data." The temperatures of the lowest transect at 29 May 11:50 A.M. to 12:20 P.M. CST are displayed in Figures 2a and 2b.

The normalized power spectrum of temperature in temporal (frequency spectrum) and spatial (wave number spectrum) domains were then calculated (Figure 2c). The wave number spectrum was divided by the mean velocity so that it corresponds to the frequency spectrum (equation (1)) [*Wyngaard and Clifford*, 1977]. Both the normalized frequency spectrum and normalized wave number spectrum were close to Kolmogorov −5/3 spectrum [*Kolmogorov*, 1941] in the inertial subrange (Figure 2c). There is a sharp jump in the right tail of the frequency spectrum because of the smoothing filter and thus due to the loss of signal at higher wave numbers. As we elaborate on later, it is noteworthy that the measured wave number spectrum is higher than the frequency spectrum at the equivalent wave numbers in the inertial subrange.

4. Results

The wave number-dependent convection velocities, computed using equation (2), normalized by the maximum convection velocity, were calculated under different stability conditions using the DTS data (Figure 3). Across stability conditions, convection velocities exhibit a ${k_1}^{-1/3}$ decrease at the higher wave numbers of the inertial subrange. The latter result emphasizes that Taylor's hypothesis does not apply in the higher wave number part of the inertial subrange and that smaller eddies are convected at smaller velocity than expected by Taylor's hypothesis. The results shown here are in agreement with observations [*Atkinson et al.*, 2015; *Chung and McKeon*, 2010; *Del Álamo and Jiménez*, 2009; *Krogstad et al.*, 1998] that low wave number components convect at larger velocities and are also consistent with findings that larger eddies are better candidates for applications of Taylors's hypothesis [*Higgins et al.*, 2012; *Mizuno and Panofsky*, 1975]. Taylor's hypothesis may thus be a good approximation for larger (i.e., energy-containing) eddies but not for

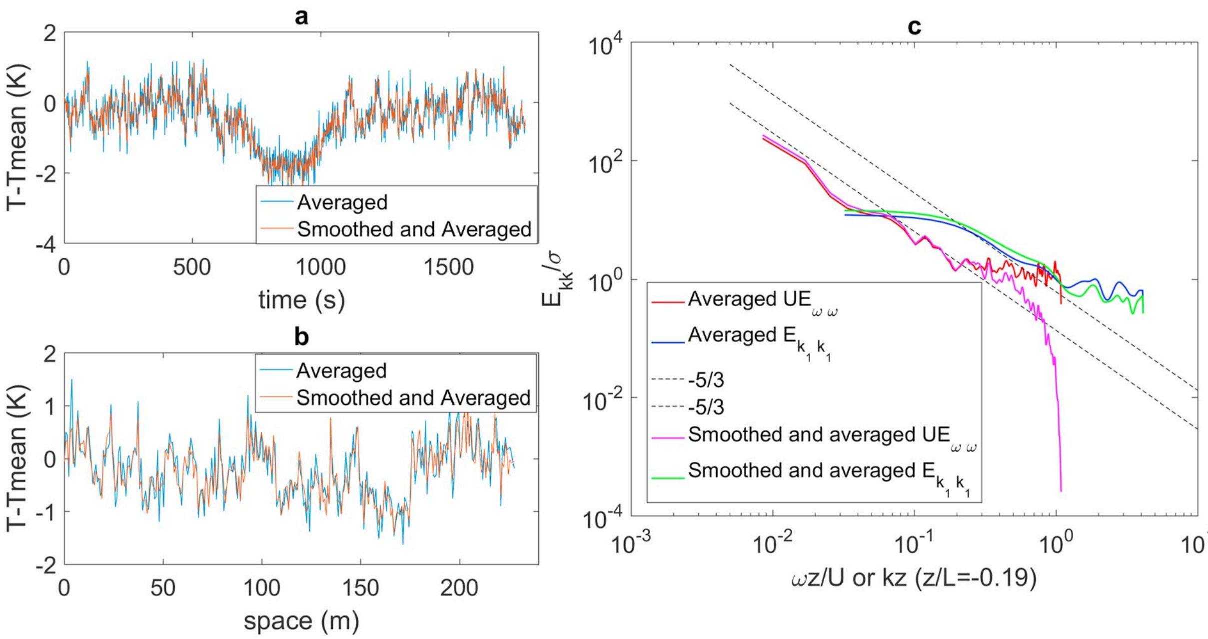

Figure 2. (a) “Averaged” and “smoothed and averaged” temporal temperature data for a fixed point in the transect. (b) “Averaged” and “smoothed and averaged” temperature along the transect for a fixed time. The *y* axis is temperature minus the mean. (c) “Averaged” and “smoothed and averaged” temperature spectrum in the time and space domain. The parameter ω is the angular frequency in the time domain, *k* is the wave number in the spatial domain, k_1 is the streamwise wave number, *z* is the optic fiber height above ground, *L* is the Obukhov length, *U* is the mean wind velocity, $E_{\omega\omega}$ is the power spectrum in frequency, E_{kk} is the power spectrum in wave number, and σ is the temperature variance of temporal or spatial data.

smaller eddies in the inertial subrange. The observed $k_1^{-1/3}$ dependence can be theoretically derived using an advection-diffusion equation with a sweeping model. Detailed derivation can be found in the supporting information [*Haller*, 2002; *Kraichnan*, 1964; *Roberts*, 1961; *Taylor*, 1938; *Tennekes*, 1975; *Wilczek and Narita*, 2012; *Wolf et al.*, 1985; *Wyngaard and Clifford*, 1977]. Indeed, eddies in the inertial subrange are governed

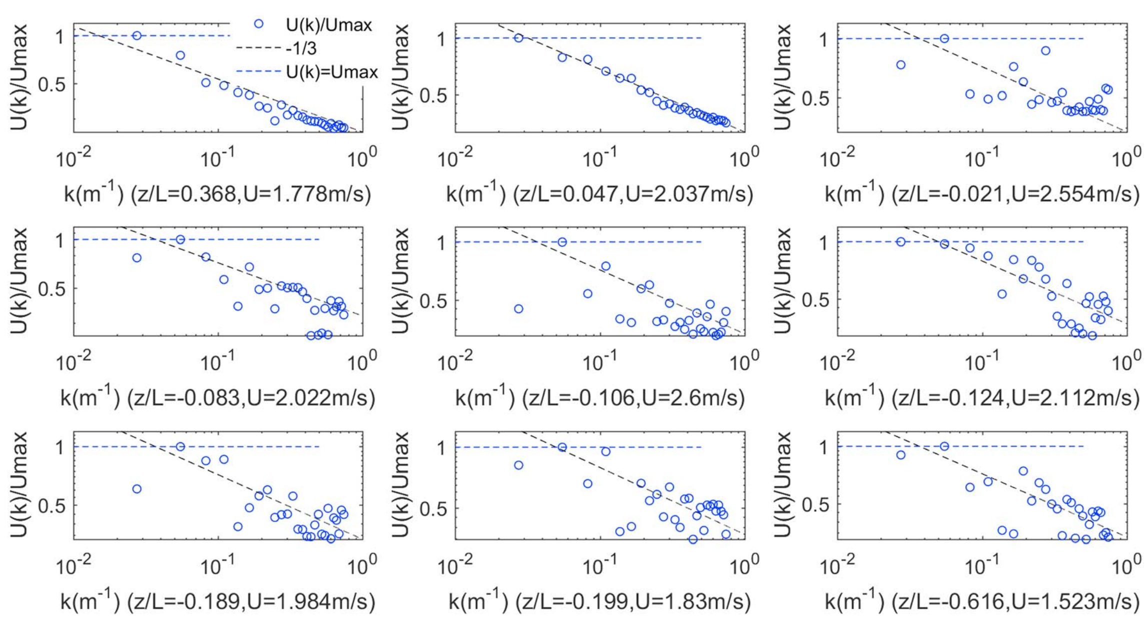

Figure 3. Ratios of different wave number components convection velocities and maximum convection velocity under different stability conditions. The parameter *z* the is optic fiber height above ground, *L* is the Obukhov length, *k* is the one-dimensional streamwise wave number, *U*(*k*) is the convection velocities of different wave number components, $U_{\max}$ is the maximum convection velocity, and *U* is the mean wind velocity. The maximum convection velocity rather than mean velocity is the denominator.

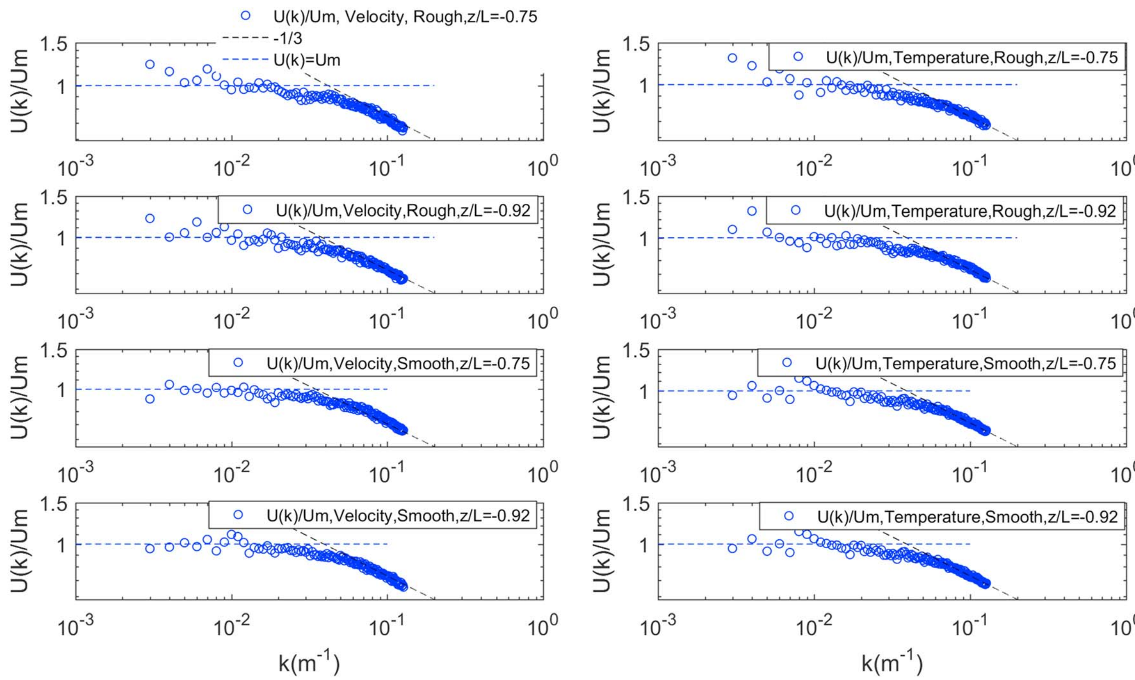

Figure 4. Ratios of different wave number components convection velocities and mean streamwise velocity of LES data. The parameter z is the vertical height of the LES data, L is the Obukhov length, k is the one-dimensional streamwise wave number, $U(k)$ is the convection velocities of different wave number components, and U_m is the mean streamwise velocity.

by the random sweeping [*Kraichnan*, 1964; *Tennekes*, 1975], mean advection at the mean streamwise velocity (consistent with Taylor's hypothesis [*Taylor*, 1938]) and turbulent diffusion [*Roberts*, 1961]. Large eddies, even in the inertial subrange, are characterized mainly by the advection and sweeping term [*Wilczek and Narita*, 2012; *Wilczek et al*., 2015]. The advection velocity leads to Doppler shift in frequency while the random sweeping velocity leads to frequency broadening [*Wilczek and Narita*, 2012] and thus to decorrelation. The decorrelation due to random sweeping nonetheless does not violate Taylor's correlation, because on average the random sweeping cancels out, and when computing the averaged spectrum, larger eddies are still advecting at the mean velocity. We thus conclude, contrary to *Higgins et al.* [2012], that decorrelation (of larger eddies) does not generate failure of Taylor's hypothesis. In fact, Taylor's hypothesis fails for smaller eddies because the turbulent diffusion term becomes large and thus because small eddies lose their coherence as they are being advected. This results in the observation of "smaller" convective velocity, which mostly reflects the dissipation of the eddy property rather than a real deceleration of the actual convective velocity. We thus conclude that it is the "frozen" assumption that is not correct in Taylor's hypothesis, because small eddies lose their coherent properties and thus their properties are not conserved. This diffusion effect generates a ${k_1}^{-1/3}$ scaling at the highest wave numbers of the inertial subrange (supporting information S1). It is thus the decoherence of small eddies that generates the deviation from Taylor's hypothesis but not the decorrelation, which is also observed for large eddies where Taylor's hypothesis still applies.

To further validate our observational and theoretical finding, we conducted similar analysis with LES data across varying stability conditions and over either a smooth or rough surface (Figure 4). The LES data were used to confirm our finding in other conditions but also to further check our results with wind data in addition to temperature data. At low wave numbers, the ratios of wave number-dependent convection velocities and maximum convection velocity tend to be constant in the LES data for both the temperature and wind velocity (downwind component) data (Figure 4), confirming that Taylor's hypothesis applies at low wave number (large eddies). A ${k_1}^{-1/3}$ convective velocity dependence is observed at large k_1, in the inertial subrange, similarly to our observations. The demarcation of the constant ratio and ${k_1}^{-1/3}$ relation is within the inertial subrange (supporting information). Therefore, we conclude that the convection velocity does not depend on wave number in the energy-containing range and at low wave numbers in the inertial subrange

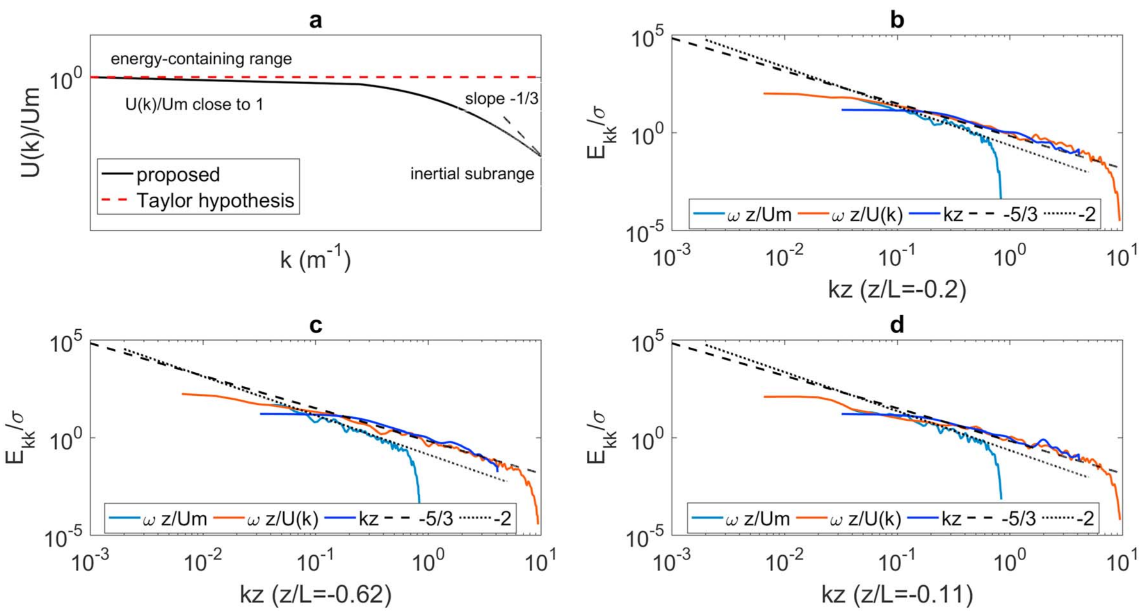

Figure 5. (a) Schematic relation between convection velocity and wave number indicated by Taylor's hypothesis and this paper. (b–d) Normalized frequency spectrum ($\omega z/U_m$), corrected normalized frequency spectrum ($\omega z/U(k)$) and measured normalized one-dimensional wave number spectrum (kz).The parameter k is the one-dimensional streamwise wave number in the spatial domain, $U(k)$ is the convection velocity of different wave number components, U_m is the mean streamwise wind velocity, ω is the angular frequency, z is the optic fiber height above ground, L is the Obukhov length, E_{kk} is the power spectrum in wave number, and σ is the temperature variance of spatial data or temporal data.

consistent with our theoretical derivation (supporting information). It exhibits a ${k_1}^{-1/3}$ decay at high wave numbers in the inertial subrange. This results applies to both momentum and scalars (Figure 4), similarly to our theoretical derivation.

In order to correct routinely available turbulent frequency data, we derive a relationship between the wave number and frequency spectra based on the observed behavior. The relation between angular frequency ω, one-dimensional wave number k_1, and convection velocity $U(k_1)$ is

$$w = k_1 U(k_1). \tag{3}$$

This can be reformulated as

$$\frac{\omega z}{\bar{U}} = \frac{k_1 U(k_1) z}{\bar{U}} = k_1 z \frac{U(k_1)}{\bar{U}}, \tag{4}$$

where $\frac{\omega z}{\bar{U}}$ and $k_1 z$ are normalized measured frequency and wave number, respectively, $\bar{U}$ is mean wind velocity. Taylor's hypothesis just assumes that $k_1 z$ can be replaced by $\frac{\omega z}{\bar{U}}$, namely,

$$k_1 z = \frac{\omega z}{\bar{U}}. \tag{5}$$

In reality, to obtain the wave number spectrum from frequency spectrum we need to use the actual wave number-dependent convective velocity:

$$k_1 z = \frac{\omega z}{\bar{U}} \frac{\bar{U}}{U(k_1)} = \frac{\omega z}{U(k_1)} \tag{6}$$

The wave number-dependent convective velocity $U(k_1)$ can then readily be calculated from the temporal frequency ω by inverting equation (4). Using this strategy, we are now in a position to correct typical temporal data spectra as available at routine eddy-covariance towers. The relation (Figure 5a) between convection velocity and wave number is as follows,

$$\frac{U(k_1)}{U_m} = \begin{cases} 1, \text{for large eddies} \\ C\left(\frac{k_1}{k_d}\right)^{-1/3}, \text{for small eddies} \end{cases} \tag{7}$$

where k_1 is the one-dimensional wave number, $U(k_1)$ is the wave number-dependent convection velocity, C is a constant coefficient smaller than 1, k_d is the starting wave number of $-1/3$ scaling in inertial subrange (supporting information), and U_m is the mean convection velocity, which is the mean streamwise velocity.

The typical normalized frequency spectrum ($\frac{\omega z}{\overline{U}}$ in equation (5)) using Taylor's hypothesis, is then compared to the corrected frequency spectrum ($\frac{\omega z}{U(k_1)}$ in equation (6)) and measured normalized wave number spectrum ($k_1 z$ in equation (6)) (Figures 5b–5d). The spectra obtained by Taylor's hypothesis systematically underestimate the energy spectra, whereas the corrected spectrum with a ${k_1}^{-1/3}$ dependence of the convective velocity at high wave numbers in the inertial subrange better reproduces the observed spatial spectrum (Figure 5b–5d). The systematic underestimation of the temporal spectrum in the temporal domain using Taylor's hypothesis (before correction) might be one of the reasons for the underestimation of turbulent energy fluxes [*Foken*, 2008] and the lack of closure at eddy-covariance sites. We calculated that the underestimation of turbulent energy in the inertial subrange is 10%–30% due to direct application of Taylor's frozen turbulence hypothesis (see details in the supporting information).

5. Conclusions

We used distributed temperature sensing and large eddy simulation (LES) data to show that Taylor's frozen turbulence hypothesis does not apply in the inertial subrange. We also derived the asymptotic advection velocity of eddies in the inertial subrange. For larger eddies in the energy-containing range and the inertial subrange, the convection velocity is constant as hypothesized by Taylor's hypothesis, but the convective velocity exhibits a ${k_1}^{-1/3}$ dependence for smaller eddies in the inertial subrange, due to the loss of eddy coherence induced by turbulent diffusion. In other words, smaller eddies appear to be convecting at lower velocities because they lose their properties as they are being advected. A correction is proposed for eddy-covariance data that can be applied to existing high-frequency temporal data. Those results should improve estimates of surface turbulent energy and CO_2 fluxes.

Acknowledgments
P.G. would like to acknowledge funding from the National Science Foundation (NSF CAREER, EAR- 1552304), and from the Department of Energy (DOE Early Career, DE-SC00142013). Selker's contributions to this work were made possible by the Center for Transformative Environmental Monitoring Programs (CTEMPs) funded by the National Science Foundation, award EAR 1440506. We would like to thank Tyson Ochsner for discussion in experiment setup. We would like to thank Nicki Hickmon, Chris Martin, Jody Martin, Michael Ritsche, George Sawyer, John Schatz, Rod Soper, David Swank, and Larry Swords of DOE's ARM SGP site for the kind help in conducting the experiment and maintaining the equipment. We are grateful to Chris Stansberry for maintaining the equipment and Jingnuo Dong for downloading RBRsolo data and installing a solar panel. We are grateful to Oklahoma Mesonet for providing the meteorological data. We would like to thank the two anonymous reviewers for very valuable comments. The data are now accessible from the following links. http://www.columbia.edu/~pg2328/Website/MOISST_DTS/ReadMe.docx and http://www.columbia.edu/~pg2328/Website/MOISST_DTS/dataOnline.rar.

References

Albertson, J. D. (1996), Large eddy simulation of land-atmosphere interaction, PhD thesis, pp. 1–185, Univ. of California, Davis.

Atkinson, C., N. A. Buchmann, and J. Soria (2015), An experimental investigation of turbulent convection velocities in a turbulent boundary layer, *Flow Turbul. Combust.*, *94*(1), 79–95, doi:10.1007/s10494-014-9582-0.

Becker, M. W., B. Bauer, and A. Hutchinson (2013), Measuring artificial recharge with fiber optic distributed temperature sensing, *Ground Water*, *51*(5), 670–678, doi:10.1111/j.1745-6584.2012.01006.x.

Bou-Zeid, E., C. Meneveau, and M. Parlange (2005), A scale-dependent Lagrangian dynamic model for large eddy simulation of complex turbulent flows, *Phys. Fluids*, *17*(2), 025105), doi:10.1063/1.1839152.

Briggs, M. A., L. K. Lautz, J. M. McKenzie, R. P. Gordon, and D. K. Hare (2012), Using high-resolution distributed temperature sensing to quantify spatial and temporal variability in vertical hyporheic flux, *Water Resour. Res.*, *48*, W02527, doi:10.1029/2011WR011227.

Burghelea, T., E. Segre, and V. Steinberg (2005), Validity of the Taylor hypothesis in a random spatially smooth flow, *Phys. Fluids*, *17*(10), 103101, doi:10.1063/1.2077367.

Buxton, O. R. H., and B. Ganapathisubramani (2011), PIV measurements of convection velocities in a turbulent mixing layer, *J. Phys. Conf. Ser.*, *318*(5), 052038), doi:10.1088/1742-6596/318/5/052038.

Buxton, O. R. H., R. de Kat, and B. Ganapathisubramani (2013), The convection of large and intermediate scale fluctuations in a turbulent mixing layer, *Phys. Fluids*, *25*(12), 125105, doi:10.1063/1.4837555.

Cancelli, D. M., M. Chamecki, and N. L. Dias (2014), A large-eddy simulation study of scalar dissimilarity in the convective atmospheric boundary layer, *J. Atmos. Sci.*, *71*(1), 3–15, doi:10.1175/jas-d-13-0113.1.

Chung, D., and B. J. McKeon (2010), Large-eddy simulation of large-scale structures in long channel flow, *J. Fluid Mech.*, *661*, 341–364, doi:10.1017/s0022112010002995.

de Kat, R., Gan, L., Dawson, J. R., and Ganapathisubramani, B. (2013), Limitations of estimating turbulent convection velocities from PIV, *arXiv preprint arXiv*, *1311.6400*.

Del Álamo, J. C., and J. Jiménez (2009), Estimation of turbulent convection velocities and corrections to Taylor's approximation, *J. Fluid Mech.*, *640*, 5–26, doi:10.1017/s0022112009991029.

Dennis, D. J. C., and T. B. Nickels (2008), On the limitations of Taylor's hypothesis in constructing long structures in a turbulent boundary layer, *J. Fluid Mech.*, *614*, 197–206, doi:10.1017/s0022112008003352.

Fisher, M. J., and P. O. A. L. Davies (1964), Correlation measurements in a non-frozen pattern of turbulence, *J. Fluid Mech.*, *18*(01), 97–116, doi:10.1017/S0022112064000076.

Foken, T. (2008), The energy balance closure problem: An overview, *Ecol. Appl.*, *18*(6), 1351–1367, doi:10.1890/06-0922.1.

Foken, T., M. Mauder, C. Liebethal, F. Wimmer, F. Beyrich, J.-P. Leps, S. Raasch, H. A. R. DeBruin, W. M. L. Meijninger, and J. Bange (2010), Energy balance closure for the LITFASS-2003 experiment, *Theor. Appl. Climatol.*, *101*(1–2), 149–160, doi:10.1007/s00704-009-0216-8.

Goldschmidt, V. W., M. F. Young, and E. S. Ott (1981), Turbulent convective velocities (broadband and wavenumber dependent) in a plane jet, *J. Fluid Mech.*, *105*, 327–345, doi:10.1017/s0022112081003236.

Haller, G. (2002), Lagrangian coherent structures from approximate velocity data, *Phys. Fluids*, *14*(6), 1851–1861, doi:10.1063/1.1477449.

Higgins, C. W., M. Froidevaux, V. Simeonov, N. Vercauteren, C. Barry, and M. B. Parlange (2012), The effect of scale on the applicability of Taylor's frozen turbulence hypothesis in the atmospheric boundary layer, *Boundary Layer Meteorol.*, *143*(2), 379–391, doi:10.1007/s10546-012-9701-1.

Kaimal, J. C., J. C. Wyngaard, Y. Izumi, and O. R. Cote (1972), Spectral characteristics of surface-layer turbulence, *Q. J. R. Meteorol. Soc.*, *98*(417), 563–589, doi:10.1002/qj.49709841707.

Kim, J., and F. Hussain (1993), Propagation velocity of perturbations in turbulent channel flow, *Phys. Fluids A*, *5*(3), 695–706, doi:10.1063/1.858653.

Kolmogorov, A. N. (1941), The local structure of turbulence in incompressible viscous fluid for very large Reynolds numbers, *Dokl. Akad. Nauk SSSR*, *30*(4), 301–305.

Kraichnan, R. H. (1964), Kolmogorov's hypotheses and Eulerian turbulence theory, *Phys. Fluids*, *7*(11), 1723–1734, doi:10.1063/1.2746572.

Krogstad, P. A., J. H. Kaspersen, and S. Rimestad (1998), Convection velocities in a turbulent boundary layer, *Phys. Fluids*, *10*(4), 949–957, doi:10.1063/1.869617.

Kumar, V., J. Kleissl, C. Meneveau, and M. B. Parlange (2006), Large-eddy simulation of a diurnal cycle of the atmospheric boundary layer: Atmospheric stability and scaling issues, *Water Resour. Res.*, *42*, W06D09, doi:10.1029/2005WR004651.

Li, Q., E. Bou-Zeid, W. Anderson, S. Grimmond, and M. Hultmark (2016), Quality and reliability of LES of convective scalar transfer at high Reynolds numbers, *Int. J. Heat Mass Transfer*, *102*, 959–970, doi:10.1016/j.ijheatmasstransfer.2016.06.093.

Lin, C. C. (1953), On Taylor's hypothesis and the acceleration terms in the Navier-Stokes equations, *Q. Appl. Math.*, *10*(4), 295–306.

Lumley, J. L. (1965), Interpretation of time spectra measured in high-intensity shear flows, *Phys. Fluids*, *8*(6), 1056–1062, doi:10.1063/1.1761355.

Mamadou, O., L. Gourlez de la Motte, A. De Ligne, B. Heinesch, and M. Aubinet (2016), Sensitivity of the annual net ecosystem exchange to the cospectral model used for high frequency loss corrections at a grazed grassland site, *Agric. For. Meteorol.*, *228*, 360–369, doi:10.1016/j.agrformet.2016.06.008.

Mizuno, T., and H. A. Panofsky (1975), The validity of Taylor's hypothesis in the atmospheric surface layer, *Boundary Layer Meteorol.*, *9*(4), 375–380, doi:10.1007/BF00223388.

Moeng, C.-H. (1984), A large-eddy-simulation model for the study of planetary boundary-layer turbulence, *J. Atmos. Sci.*, *41*(13), 2052–2062.

Monin, A., and A. Obukhov (1954), Basic laws of turbulent mixing in the surface layer of the atmosphere, *Contrib. Geophys. Inst. Acad. Sci. USSR*, *151*(163), e187.

Mueller, B., et al. (2013), Benchmark products for land evapotranspiration: LandFlux-EVAL multi-data set synthesis, *Hydrol. Earth Syst. Sci.*, *17*(10), 3707–3720, doi:10.5194/hess-17-3707-2013.

Mueller, B., et al. (2011), Evaluation of global observations-based evapotranspiration datasets and IPCC AR4 simulations, *Geophys. Res. Lett.*, *38*, L06402, doi:10.1029/2010GL046230.

Porté-Agel, F., C. Meneveau, and M. B. Parlange (2000), A scale-dependent dynamic model for large-eddy simulation: Application to a neutral atmospheric boundary layer, *J. Fluid Mech.*, *415*, 261–284, doi:10.1017/s0022112000008776.

Powell, D. C., and C. E. Elderkin (1974), An investigation of the application of Taylor's hypothesis to atmospheric boundary layer turbulence, *J. Atmos. Sci.*, *31*(4), 990–1002, doi:10.1175/1520-0469(1974)031<0990:AIOTAO>2.0.CO;2.

Roberts, P. H. (1961), Analytical theory of turbulent diffusion, *J. Fluid Mech.*, *11*(02), 257–283, doi:10.1017/s0022112061000500.

Sayde, C., C. Thomas, J. Wagner, and J. Selker (2015), High-resolution wind speed measurements using actively heated fiber optics, *Geophys. Res. Lett.*, *42*, 10,064–10,073, doi:10.1002/2015GL066729.

Selker, J., N. van de Giesen, M. Westhoff, W. Luxemburg, and M. B. Parlange (2006a), Fiber optics opens window on stream dynamics, *Geophys. Res. Lett.*, *33*, L24401, doi:10.1029/2006GL027979.

Selker, J., L. Thévenaz, H. Huwald, A. Mallet, W. Luxemburg, N. van de Giesen, M. Stejskal, J. Zeman, M. Westhoff, and M. B. Parlange (2006b), Distributed fiber-optic temperature sensing for hydrologic systems, *Water Resour. Res.*, *42*, W12202, doi:10.1029/2006WR005326.

Sullivan, P. P., and E. G. Patton (2011), The effect of mesh resolution on convective boundary layer statistics and structures generated by large-Eddy simulation, *J. Atmos. Sci.*, *68*(10), 2395–2415, doi:10.1175/jas-d-10-05010.1.

Taylor, G. I. (1938), The spectrum of turbulence, *Proc. R. Soc. London A*, *164*(919), 476–490.

Tennekes, H. (1975), Eulerian and Lagrangian time microscales in isotropic turbulence, *J. Fluid Mech.*, *67*(03), 561–567, doi:10.1017/s0022112075000468.

Thomas, C. K., A. M. Kennedy, J. S. Selker, A. Moretti, M. H. Schroth, A. R. Smoot, N. B. Tufillaro, and M. J. Zeeman (2011), High-resolution fibre-optic temperature sensing: A new tool to study the two-dimensional structure of atmospheric surface-layer flow, *Boundary Layer Meteorol.*, *142*(2), 177–192, doi:10.1007/s10546-011-9672-7.

Tong, C. (1996), Taylor's hypothesis and two-point coherence measurements, *Boundary Layer Meteorol.*, *81*(3–4), 399–410, doi:10.1007/BF02430337.

Tyler, S. W., J. S. Selker, M. B. Hausner, C. E. Hatch, T. Torgersen, C. E. Thodal, and S. G. Schladow (2009), Environmental temperature sensing using Raman spectra DTS fiber-optic methods, *Water Resour. Res.*, *45*, W00D23, doi:10.1029/2008WR007052.

Wilczek, M., and Y. Narita (2012), Wave-number-frequency spectrum for turbulence from a random sweeping hypothesis with mean flow, *Phys. Rev. E*, *86*(6), 066308), doi:10.1103/PhysRevE.86.066308.

Wilczek, S., J. A. M. Richard, and C. Meneveau (2015), Spatio-temporal spectra in the logarithmic layer of wall turbulence: Large-eddy simulations and simple models, *J. Fluid Mech.*, *769*, 1–12, doi:10.1017/jfm.2015.116.

Wills, J. A. B. (1964), On convection velocities in turbulent shear flows, *J. Fluid Mech.*, *20*(03), 417–432, doi:10.1017/s002211206400132x.

Wolf, A., J. B. Swift, H. L. Swinney, and J. A. Vastano (1985), Determining Lyapunov exponents from a time series, *Phys. D*, *16*(3), 285–317, doi:10.1016/0167-2789(85)90011-9.

Wyngaard, J. C., and S. F. Clifford (1977), Taylor's hypothesis and high-frequency turbulence spectra, *J. Atmos. Sci.*, *34*(6), 922–929.

Zeeman, M. J., J. S. Selker, and C. K. Thomas (2015), Near-surface motion in the nocturnal, stable boundary layer observed with fibre-optic distributed temperature sensing, *Boundary Layer Meteorol.*, *154*(2), 189–205, doi:10.1007/s10546-014-9972-9.

Zhao, X., and G. W. He (2009), Space-time correlations of fluctuating velocities in turbulent shear flows, *Phys. Rev. E*, *79*(4), 046316), doi:10.1103/PhysRevE.79.046316.